Self-Organization of Hairy-Rod Polymers

R. Stepanyan,[†] A. Subbotin,[†,‡] M. Knaapila,[§] O. Ikkala,[§] and G. ten Brinke*[,†,§]

Department of Polymer Science and Material Science Center, University of Groningen, Nijenborgh 4, 9747 AG Groningen, The Netherlands; Institute of Petrochemical Synthesis, Russian Academy of Sciences, Moscow 119991, Russia; and Department of Engineering Physics and Mathematics, Helsinki University of Technology, P.O. Box 2200, FIN-02015 HUT, Espoo, Finland

Received December 16, 2002; Revised Manuscript Received March 20, 2003

ABSTRACT: Self-organized structure formation in the melt of hairy-rod polymers is analyzed theoretically. It is shown that the interplay between unfavorable repulsive rod−coil interactions and stretching of the side chains is responsible for the appearance of three different microphases: one lamellar and two hexagonal. The first-order phase transitions between these are considered in detail. If the side chains are long enough for the elastic stretching free energy to dominate the repulsive interactions, hexagonally ordered domains of hairy-rod cylindrical brushes are formed. The lamellar phase is shown to be stable for shorter side chains and occupies an important part of the phase diagram. In the intermediate side chain length regime another hexagonally ordered structure appears, characterized by cylindrical micelles with an elongated cross section, containing several hairy-rod polymers.

1. Introduction

Hairy-rod polymers[1−3] consist of rigid backbones with a dense system of side chains. As other block copolymers, they tend to self-organize, forming nanoscale structures in bulk and in solutions. In particular, in the context of electrical conductivity such architectures received a lot of attention (see ref 4 and references therein), since there the backbones consist of conjugated rigid polymers. Besides block copolymeric self-organization, there is an even more important reason why hairy rods have attracted so much interest. In general, rigid-rod-like polymers do not melt and dissolve only poorly, if at all, in common solvents due to a strong aggregation tendency and a small gain of conformational entropy upon dissolution or melting. By covalent connection of substituent groups (notably flexible alkyl chains) to the backbone, a system is achieved where the rigid polymer can be regarded to dissolve in the background of the side chains due to the (infinite) attractive interaction between the solvent molecules and the backbone. This causes melting point depression[5,6] without loss of rigidity of the backbone.[1] In this way fusibility can be achieved and higher solubility in an organic solvent, to allow melt and solution processability. The nature and length of the covalently bonded side chains have a large effect on the phase behavior. A wide variety of different modifications exist, depending on the selection of the backbone and side chains (see the reviews by Ballauff [1] and Menzel[2]).

Unsubstituted rigid-rod polymers have typically a high melting temperature, e.g., ca. 600 °C for the polyester poly(1,4-phenylene 2,5-di-*n*-alkoxy terephthalate) with side chain length $n = 0$. However, even a short alkyl tail of length $2 < n \leq 6$ reduces substantially the melting temperature (to 250−300 °C), and a transition from a crystalline to a nematic phase is reported for the above-mentioned polyester.[1,7] For longer side chains, the melting point is reduced further; for example, for $n = 12$ it is 150 °C. However, as the nonpolar side chains become longer, i.e., $n \geq 8$, the repulsion with the backbone becomes correspondingly larger. Therefore, one enters into the regime of self-organization, where the alkyl tails and the backbones microphase-separate, and a layered structure is formed.[1,3,7−10]

A literature survey shows that in most cases the self-organization is in the form of lamellar structures. For example, the self-organized structures in bulk of alkyl-substituted polythiophenes have been systematically studied by Winokur et al.[11] and Chen et al.,[12] demonstrating the formation of self-organized lamellar phases for $n \geq 4$. A further example concerns poly(*p*-phenylene) (PPP), which is an insoluble and infusible conjugated polymer. On the basis of this polymer, Wegner et al. prepared several different types of hairy rods.[13−15] Poly-(2,5-di-*n*-dodecyl-1,4-phenylene) contains two flexible alkyl tails at each aromatic ring.[14] In the solid state a self-organized lamellar phase is obtained with a long period of ca. 35 Å at room temperature. Upon heating, the long period slightly decreases until at ca. 190 °C an ODT to a disordered state occurs. A modification is reported where the alkyl side chains have been replaced by alkoxy chains.[15] For octyloxy and dodecyloxy side chains ($n = 8$, 12), lamellar self-organized structures are obtained. However, for shorter butoxy or pentoxy tails ($n = 4$, 5) the distribution of side chains around the polymer backbone was described as approximately cylindrical. These side chains are probably too short to induce microphase separation.

Hairy-rod architecture involving polyaniline with covalently bonded side chains is yet another example. The emeraldine base (EB) form of polyaniline consists of alternating amine and imine repeat units. Side chains have been introduced by covalent connection of short alkyl (methyl or ethyl) chains to the aromatic rings[16] or by a series of different long alkyl chains ranging from butyl to octadecyl to the aminic nitrogens.[17] Levon et al.[18] prepared N-alkylated polyaniline starting from

[†] University of Groningen.
[‡] Russian Academy of Sciences.
[§] Helsinki University of Technology.
* Corresponding author.

10.1021/ma0259665 CCC: $25.00
Published on Web 04/15/2003

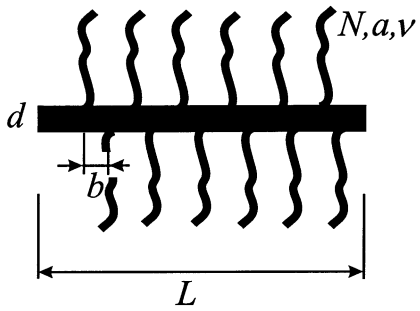

Figure 1. Model of the hairy rod.

leucoemeraldine, the completely reduced form of polyaniline. Products with octyl or longer side chains showed strongly improved solubility in common organic solvents such as chloroform, toluene, etc. In the bulk state self-organized layered structures are formed with a long period linearly increasing from ca. 20 to 32 Å as a function of the side chain length.[18]

Many more examples[19] can be given, all demonstrating that bulk systems consisting of hairy-rod polymers self-organize due to microphase separation between the backbone and the side chains if the side chains are long enough. In almost all cases a layered structure is found. It should, however, be realized that in all cases the length of the side chains involved is relatively small. The opposite case of a dense set of very long side chains has received a lot of attention lately in the case of flexible backbones, the so-called "molecular bottle brushes".[20−23] Still the experimental data on these systems are of some interest in relation to hairy-rod molecules, since the presence of long side chains in the case of flexible backbone leads to very stiff cylindrical structures. Most studies concern dilute solution properties. In one paper dealing with polymacromonomers consisting of a polymethacrylate main chain and polystyrene side chains in toluene, the influence of the concentration was addressed, and a lyotropic phase formed by individual molecules was reported at elevated concentrations (31.5 wt %).[20]

It is the objective of this work to address theoretically the microstructure formation driven by the repulsion between the stiff polymer backbone and the flexible side chains of any length.

2. The Model

We consider a melt of hairy-rod polymers with a backbone of length L and diameter d ($L \gg d$) bearing M flexible side chains equidistantly grafted with a density $1/b$ ($b = L/M$) as depicted in Figure 1. Each side chain is a coil consisting of N beads of volume ν and statistical segment length a, so that the unperturbed coil size is $R_c = a\sqrt{N}$ (here we assume $R_c \ll L$). This implies that the composition f, volume fraction of the backbone, is related to the side chain length by $f = 1/(1 + \kappa N)$, where $\kappa = \nu/(\pi d^2 b/4)$ is the ratio between the volume of a side chain bead and the volume of the backbone between two successive side chains.

In the limiting case of $N = 0$ (no side chains) the system obviously forms a nematic phase consisting of strongly oriented backbones, which have orientational free energy[24,25] $\mathcal{F}_{or}^{Nem} \simeq T \ln(4\pi/\Omega_0)$, where Ω_0 is the characteristic fluctuation angle.

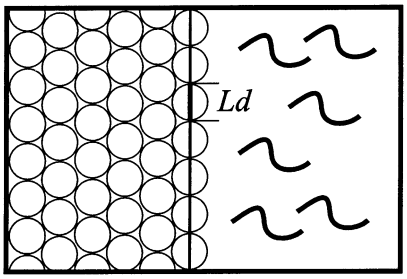

Figure 2. Illustration of the interface free energy calculation.

In the presence of side chains each rod is surrounded by flexible coils. The interaction between rods and coils can be introduced in the following way. If both were *not* linked to each other, they would macrophase-separate into almost pure phases with a sharp interface in between (Figure 2) so that virtually no coils are present in the rod-rich phase and vice versa.[26,27] The interface is characterized by interface tension γ. To define the interfacial energy for one rod surrounded by flexible coils, we use the following approximation

$$\mathcal{F}_{\gamma}^{(1)} \simeq 2Ld\gamma \tag{1}$$

where the prefactor 2 reflects the fact that the rod's contact area is twice as large as in the case of the flat interface (see Figure 2). The interfacial tension γ is related to the conventional Flory−Huggins χ-parameter and can be calculated analytically under certain conditions.[28,29] Here we treat γ as known and also assume $\lim_{T\to\infty} \gamma/T = \Gamma_\infty > 0$.

In general, the free energy of the hairy-rod system, i.e., covalently bonded rods and coils, can be written as a sum of three terms (per molecule):

$$\mathcal{F} = \mathcal{F}_{\gamma} + \mathcal{F}_{el} + \delta\mathcal{F}_{or} \tag{2}$$

Here we take as a reference state the corresponding sum of the free energies of the pure nematic phase and the pure melt of flexible coils. Therefore, the last term can be expressed as $\delta F_{or} \simeq T \ln(\Omega_0/\Omega)$. Since the new characteristic fluctuation angle Ω is close to Ω_0, $\delta\mathcal{F}_{or}$ is small (in all phases we consider here backbones are aligned). In this way, the free energy of the system consists of the rod−coil interfacial tension $\mathcal{F}_{\gamma}$ part and the elastic stretching energy of the side chains $\mathcal{F}_{el}$:

$$\mathcal{F} = \mathcal{F}_{\gamma} + \mathcal{F}_{el} \tag{3}$$

Because of unfavorable interaction between rods and coils, the system tends to form rod- and coil-rich domains. Depending on the geometry of these domains, also the energy of elastic stretching is changed. Thus, the interplay between $\mathcal{F}_{\gamma}$ and $\mathcal{F}_{el}$ determines which geometry of the micelle (e.g., cylindrical or lamellar) is more favorable.

3. Phase Equilibria between Microphases and Nematic

In this section we address the question about the different phases that can appear in the melt. Let us start from a relatively small γ/T (or large N), such that the elastic stretching plays the dominant role. Then the cylindrical micelles will contain a single hairy-rod molecule in its cross section. The cylinders should be

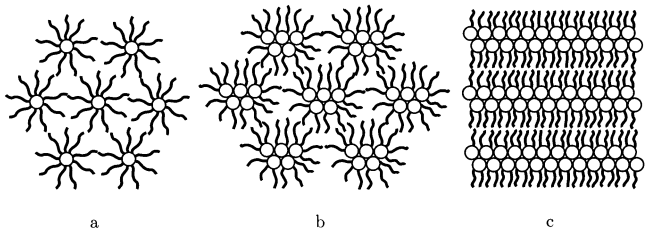

Figure 3. Possible microstructures: (a) hexagonal H1; (b) hexagonal H2; (c) lamellar.

closely packed and thus arranged in a hexagonal lattice (Figure 3). In the opposite case of very high γ/T the elastic stretching is negligible. Therefore, to decrease the $\mathcal{F}_\gamma$ contribution, the system adopts a layered structure (Figure 3) with each lamella being a double layer of rods. In the intermediate regime another hexagonal structure H2 with $Q > 1$ molecules per micelle may be realized (Figure 3).

In the following subsections we address the competition and coexistence between these phases quantitatively.

3.1. Hexagonal H1 Phase. Here we start from the relatively small γ and large $\kappa N \gg 1$ case. Then the backbone occupies only a small fraction of the total molecule's volume; i.e., each hairy rod forms a densely grafted cylindrical brush. To fill space, these brushes reside in a hexagonal lattice (Figure 3). The free energy of the system equals $\mathcal{F}_{H1} = \mathcal{F}_\gamma + \mathcal{F}_{el}$ where the first term is $\mathcal{F}_\gamma \simeq 2Ld\gamma$ due to the fact that each rod is completely surrounded by coils.

The elastic stretching energy of the side chains can be calculated by the method presented in refs 30 and 31 and reads

$$\mathcal{F}_{el} = T\frac{3\kappa d^2}{32a^2} M \ln(\kappa N) \tag{4}$$

In expression eq 3 we omitted the loss of translational energy and the interaction between the hairy-rod polymers because both are relatively small. The latter arises from the free ends distribution, which leads to penetration of the side chain ends belonging to one hairy-rod polymer into the coronas of its neighbors.[28]

At this point it is useful to introduce a renormalized free energy $\tilde{F} = \mathcal{F}/(MT)$. For the hexagonal phase consisting of separate hairy-rod cylindrical brushes, called hexagonal H1, this free energy equals

$$\tilde{F}_{H1} = 2\frac{bd\gamma}{T} + \frac{3d^2}{32a^2}\kappa \ln(\kappa N) \tag{5}$$

This expression allows us to identify the condition under which H1 will be found. It corresponds to the situation where the elastic tension of the side chains is larger than the "interfacial term" so that the rods are prevented from sticking together.

The lattice parameter l can be estimated from the volume fraction condition $f \sim d^2/l^2$ and reads

$$l \sim d/\sqrt{f} \tag{6}$$

3.2. Hexagonal H2 Phase. An increase of the γ/T parameter results in a tendency of the backbones to adopt a packing with a smaller total area of contact with side chains (Figure 3). Assuming that the coils cannot penetrate into the core of a cylindrical H2 type micelle, the core must have a double-layer structure of closely packed backbones with surface $QdL + 2dL$ (valid for $Q \geq 2$), where the second addend is due to edges. For a core size smaller than the corona thickness, i.e., $Q < \sqrt{N}$, the micelles still have an approximately circular cross section so that in a good approximation eq 4 with a renormalized grafting density can be used for the elastic stretching. Therefore, the free energy per molecule in the H2 phase is given by

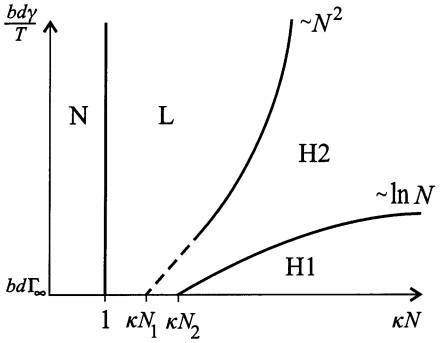

Figure 4. Phase diagram of the melt of hairy-rod molecules. H1−H2 coexistence line is given by eq 10; H2−L (solid part) corresponds to eq 19.

$$\tilde{F}_{H2} = \frac{bd\gamma}{T}\left(1 + \frac{2}{Q}\right) + \frac{3d^2}{32a^2}\kappa Q \ln(\kappa N) \tag{7}$$

and the number of rods per unit cell Q follows from the minimization $\partial\tilde{F}_{H2}/\partial Q = 0$, i.e.

$$Q = \sqrt{\frac{2bd\gamma/T}{\frac{3d^2}{32a^2}\kappa \ln(\kappa N)}} \tag{8}$$

This yields the following expression for the free energy of the hexagonal H2 phase under the condition that the cylinders have a cross section that is still quite close to circular

$$\tilde{F}_{H2} = \frac{bd\gamma}{T} + 2\sqrt{\frac{2bd\gamma}{T}\frac{3d^2}{32a^2}\kappa \ln(\kappa N)} \tag{9}$$

At this point the first-order H1−H2 transition can be identified and its temperature obtained from the comparison of eq 5 and eq 9. It gives the following equation for the H1−H2 coexistence line presented in Figure 4:

$$\frac{bd\gamma}{T} = (3 + 2\sqrt{2})\frac{3d^2}{32a^2}\kappa \ln(\kappa N) \tag{10}$$

Using eq 8, we conclude that the average number of molecules per micelle of length L is $Q_1 = 2 + \sqrt{2} \simeq 3.4$ when H2 first appears. Hence, the cylindrical domain has 3−4 backbones in its cross section. This small number is consistent with the approximation used concerning the almost circular cross section. The period of the structure is of the order of $l \sim d\sqrt{Q/f}$.

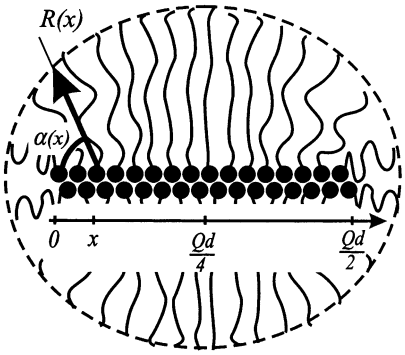

Figure 5. Cross section of a hexagonal H2 phase cylindrical micelle in the vicinity of the H2−Lam transition. Note the total cross section is still close to circular.

3.3. Equilibrium between Lamellar and Hexagonal H2 Phase. Following the same reasoning as before, one concludes that at high enough γ/T values a lamellar phase should appear. Apparently, it is the one with minimal rod−coil contact area. Its free energy is given by

$$\tilde{F}_{\mathrm{L}} = \frac{bd\gamma}{T} + \frac{3d^2}{32a^2}\pi^2\kappa^2 N \tag{11}$$

where the second term represents the elastic stretching of the side chains. It can be easily obtained from the stretching free energy of a coil in a dense planar-brush[32,33] $F_1 = 3TH^2/(2Na^2)$. Here

$$H = \pi d\kappa N/4 \tag{12}$$

is the thickness of the side chain layer corresponding to one lamella.

The lamellar−hexagonal H2 transition condition is obtained by equating the free energies of the lamellar phase eq 11 and the hexagonal phase. However, eq 9 is not suitable for this purpose since it was written under the assumption that the H2-phase micellar core has almost circular cross section. This is definitely not the case anymore in the vicinity of the L−H2 transition (see Figure 5). The elastic part of the free energy cannot be approximated by an eq 4 type expression but should rather be calculated starting from a planar sheet and introducing appropriate edge corrections. The essential element of our approach[29] is the assumption that, in the framework of the Alexander−de Gennes approximation,[34] all chains propagate outward along *straight* lines. Near the edges of the micelle these lines are tilted with an angle $\alpha(x)$ (see Figure 5). The free end of the chain is located at the distance $R(\alpha)$ along this line. The two functions are related through the incompressibility condition

$$\frac{\mathrm{d}\alpha}{\mathrm{d}x} = \frac{2}{R^2}(H - R\sin\alpha) \tag{13}$$

Here H is the end-to-end distance of the coil far from the edge, i.e., given by eq 12, and x is the distance from the edge of the core consisting of backbones.

From this the free energy of one stretched coil can be derived (see ref 29 for details)

$$F_1 = \frac{3T}{2}\frac{\nu}{a^2bd}\frac{\ln\left(1 + R\dfrac{\mathrm{d}\alpha/\mathrm{d}x}{\sin\alpha}\right)}{\mathrm{d}\alpha/\mathrm{d}x} \tag{14}$$

and the total edge correction per one hairy rod reads

$$\mathcal{F}_{\mathrm{edges}} = \frac{4MT}{Qd}\int_0^{Qd/4}(F_1(x) - F_{1\infty})\,\mathrm{d}x \tag{15}$$

where $F_{1\infty} = \lim_{x\to\infty} F_1 = 3\nu H/(2a^2bd)$. Using eqs 13−15, this correction can be written in the form (cf. eq 33 from ref 29)

$$\mathcal{F}_{\mathrm{edges}} = \frac{6MT}{Qd}\frac{\nu H^2}{a^2bd^2}\int_0^{\pi/2}\frac{\rho^2\,\mathrm{d}\alpha}{2(1-\rho\sin\alpha)}\left[\frac{\rho^2\ln\left(\dfrac{2}{\rho\sin\alpha} - 1\right)}{2(1-\rho\sin\alpha)} - 1\right] \tag{16}$$

with a new function $\rho(\alpha) = R(x(\alpha))/H$, which should be found from numerical minimization. As it turns out, at the minimum the integral has a value of approximately $^1/_2$ and as a result

$$\mathcal{F}_{\mathrm{edges}} \simeq -T\frac{3d^2}{32a^2}\frac{\pi^3\kappa^3N^2M}{2Q} \tag{17}$$

Therefore, the elastic free energy of the H2 phase *near* the H2 to lamellar phase transition is approximately equal to

$$\tilde{F}'_{\mathrm{H2}}{}^{(\mathrm{el})} = \frac{3d^2}{32a^2}\pi^2\kappa^2N - \frac{3d^2}{32a^2}\frac{\pi^3\kappa^3N^2}{2Q} \tag{18}$$

and the total free energy now reads

$$\tilde{F}'_{\mathrm{H2}} = \frac{bd\gamma}{T}\left(1 + \frac{1}{Q}\right) + \tilde{F}'_{\mathrm{H2}}{}^{(\mathrm{el})}$$

Using the equilibrium condition $\tilde{F}_{\mathrm{L}} = \tilde{F}'_{\mathrm{H2}}$, we arrive at the expression for the lamellar−hexagonal H2 coexistence line

$$\frac{bd\gamma}{T} = \frac{3d^2}{32a^2}\frac{\pi^3\kappa^3N^2}{4} \tag{19}$$

Note that the number of rods per cylinder in the H2 phase dropped out from the result eq 19 *without* minimization. This fact is connected to the approximation eq 18, which in a sense can be viewed as an expansion in the small parameter $1/Q$. So, to obtain the number of rods Q_2 at the H2−Lam transition consistently, one has to extend the approximation eq 18. However, Q_2 can be also estimated from eq 18 when the edge correction becomes of the order of the main term

$$Q_2 \sim \kappa N \tag{20}$$

3.4. Equilibrium between Nematic and Lamellar Phases. In section 2 we started from the $\kappa N \gg 1$ case. The phase equilibrium line between the two hexagonal phases obtained, eq 10, can be extrapolated into the $\kappa N \gtrsim 1$ region. This gives for the transition point in the $T \to \infty$ limit (see Figure 4)

$$\kappa N_2 \simeq \exp\left[\frac{32ba^2\Gamma_\infty}{3(3+\sqrt{2})\kappa d}\right] \tag{21}$$

The H2−L coexistence line is prolonged into the region

of $\kappa N \gtrsim 1$ as well, yielding in the same limit

$$\kappa N_1 \simeq \sqrt{\frac{128ba^2\Gamma_\infty}{3\pi^3\kappa d}} \tag{22}$$

for $\Gamma_\infty > \Gamma_\infty^* = 3\pi^3\kappa d/(128ba^2)$. Unfortunately, no simple extrapolation can be made in the $\Gamma_\infty < \Gamma_\infty^*$ case.

Hence, only the case $\kappa N < 1$ has not been considered yet. This regime is characterized by a small fraction of side chains, implying that most probably a nematicly ordered structure should appear. We introduced the γ-part of the free energy assuming that a domain of backbones (cylindrical or lamellar) is immersed in a flexible surrounding (see eq 1). In the $\kappa N \ll 1$ case the situation is reversed: now the coils form the minority component, occupying the empty spaces in between rodlike backbones. Let us assume that one coil in the bulk of the nematic phase loses an energy

$$\mu_c \simeq 2\sigma N\gamma \tag{23}$$

where σ is a characteristic cross section area of a monomer, $\sigma \sim \nu^{2/3}$. Then the energy of the nematic phase can be written as

$$\tilde{F}_N = 2\sigma N\frac{\gamma}{T} \tag{24}$$

where we omitted the translational entropy term because of its smallness.

Now we keep γ/T constant and gradually increase the length of the side chains, so that κN approaches unity. Because of the increasing volume fraction of the coils in the system, at certain point around $\kappa N \sim 1$ a microscopically segregated state, notably lamellar, has to become favorable (see Figure 4).

It is hardly possible to make more a quantitative prediction within the framework of the simple model discussed. For this purpose expressions are needed for the nematic and the lamellar phase in the very vicinity of $\kappa N = 1$. Therefore, the line separating N and L regions in Figure 4 should be considered a qualitative estimation rather than a quantitative result.

4. Discussion and Concluding Remarks

In this paper we have shown that a melt of hairy-rod polymers exhibits interesting phase behavior resulting from the balance between unfavorable rod−coil interaction and elastic stretching of the side chains. The main results are summarized in the phase diagram Figure 4. We showed that for long enough ($\kappa N > 1$) side chains the hairy-rod polymers tend to self-organize and form microstructures. Depending on the temperature or, equivalently, on the strength of the rod−coil repulsion parameter, the system finds itself in one of three possible microphases. At relatively high temperatures hexagonally ordered domains are formed (regions H1 and H2 in Figure 4) with one or several molecules per cylindrical micelle. This is explained to be a consequence of the relatively weak repulsion between rigid and flexible polymer, which cannot outweigh the elastic stretching part of the free energy. A prominent place in the phase diagram belongs to the lamellar morphology. In the case of long side chains ($\kappa N \gg 1$) it is proven to be stable for low enough temperatures where the surface tension term starts to play the decisive role.

For somewhat shorter side chains the lamellar phase becomes the only possible one, implying that no hexagonal structures can be found in this region. This serves as a possible explanation for the fact that the lamellar phase has been found experimentally in the majority of cases studied, where the side chains are relatively short.[1,3,7,10,11,14,35,36]

In the last part of the paper we argued that a nematic phase should appear for $\kappa N < 1$. In practice, this might correspond to either a nematic or a crystalline phase.

Several experiments[14,36] report order−disorder transitions. However, this transition lies beyond our approach due to the assumption about absence of rotational disordering (see e.g. eq 2) used in the discussion from the very beginning.

Acknowledgment. A.S. acknowledges INTAS (Grant INTAS-2000-00278) and the Netherlands Organisation for Scientific Research (NWO) for support.

References and Notes

(1) Ballauff, M. *Angew. Chem., Int. Ed. Engl.* **1989**, *28*, 253.
(2) Menzel, H. In *Polymer Materials Encyclopedia*; Salamone, J. C., Ed.; CRC Press: Boca Raton, FL, 1996.
(3) Wegner, G. *Thin Solid Films* **1992**, *216*, 105.
(4) Ikkala, O.; ten Brinke, G. Self-Organized Supramolecular Polymer Structures to Control Electrical Conductivity. In *Handbook of Advanced Electronic and Photonic Materials and Devices, Part 8 Conducting Polymers*; Nalwa, H. S., Ed.; Academic Press: San Diego, 2000.
(5) Majnusz, J.; Catala, J. M.; Lenz, R. W. *Eur. Polym. J.* **1983**, *19*, 1043.
(6) Krigbaum, W. R.; Hakemi, H.; Kotek, R. *Macromolecules* **1985**, *18*, 965.
(7) Ballauff, M. *Makromol. Chem.* **1986**, *7*, 407.
(8) Galda, P.; Kistner, D.; Martin, A.; Ballauff, M. *Macromolecules* **1993**, *26*, 1595.
(9) Steuer, M.; Hörth, M.; Ballauff, M. *J. Polym. Sci., Part A: Polym. Chem.* **1993**, *31*, 1609.
(10) Ballauff, M.; Schmidt, G. F. *Makromol. Chem.* **1987**, *8*, 93.
(11) Winokur, M. J.; Wamsley, P.; Moulton, J.; Smith, P.; Heeger, A. J. *Macromolecules* **1991**, *24*, 3812.
(12) Chen, S.-A.; Ni, J.-M. *Macromolecules* **1992**, *25*, 6081.
(13) Lauter, U.; Meyer, W. H.; Wegner, G. *Macromolecules* **1997**, *30*, 2092.
(14) McCarthy, T. F.; Witteler, H.; Pakula, T.; Wegner, G. *Macromolecules* **1995**, *28*, 8350.
(15) Vahlenkamp, T.; Wegner, G. *Macromol. Chem. Phys.* **1994**, *195*, 1933.
(16) Wei, Y.; Focke, W. W.; Wnek, G. E.; Ray, A.; MacDiarmid, A. G. *J. Phys. Chem.* **1989**, *93*, 495.
(17) Zheng, W.-Y.; Levon, K.; Taka, T.; Laakso, J.; Österholm, J.-E. *J. Polym. Sci., Part B: Polym. Phys.* **1994**, *33*, 1289.
(18) Zheng, W.-Y.; Levon, K.; Laakso, J.; Österholm, J.-E. *Macromolecules* **1994**, *27*, 7754.
(19) Yu, S. M.; Tirrel, D. A. *Biomacromolecules* **2000**, *1*, 310.
(20) Wintermantel, M.; Fischer, K.; Gerle, M.; Ries, R.; Schmidt, M.; Kajiwara, K.; Urakawa, H.; Wataoka, I. *Angew. Chem., Int. Ed. Engl.* **1995**, *34*, 1472.
(21) Gerle, M.; Fischer, K.; Roos, S.; Müller, A. H. E.; Schmidt, M.; Sheiko, S. S.; Prokhorova, S.; Möller, M. *Macromolecules* **1999**, *32*, 2629.
(22) Fischer, K.; Schmidt, M. *Macromol. Rapid Commun.* **2001**, *22*, 787.
(23) Lecommandoux, S.; Chécot, F.; Borsali, R.; Schappacher, M.; Deffieux, A. *Macromolecules* **2002**, *35*, 8878.
(24) Khokhlov, A. R. Theories Based on the Onsager Approach. In *Liquid Crystallinity in Polymers*; Ciferri, A., Ed.; VCH Publishers: New York, 1991.
(25) Semenov, A. N.; Khokhlov, A. R. *Sov. Usp. Fiz. Nauk* **1988**, *156*, 427.
(26) Flory, P. J. *Macromolecules* **1978**, *11*, 1138.

(27) Abe, A.; Ballauff, M. The Flory Lattice Model. In *Liquid Crystallinity in Polymers*; Ciferri, A., Ed.; VCH Publishers: New York, 1991.
(28) Semenov, A. N. *Sov. Phys. JETP* **1985**, *61*, 733.
(29) Semenov, A. N.; Nyrkova, I. A.; Khokhlov, A. R. *Macromolecules* **1995**, *28*, 7491.
(30) Subbotin, A.; Saariaho, M.; Ikkala, O.; ten Brinke, G. *Macromolecules* **2000**, *33*, 3447.
(31) Stepanyan, R.; Subbotin, A.; ten Brinke, G. *Macromolecules* **2002**, *35*, 5640.
(32) Grosberg, A. Y.; Khokhlov, A. R. *Statistical Physics of Macromolecules;* American Institute of Physics: New York, 1994.
(33) de Gennes, P. G. *Scaling Concepts in Polymer Physics;* Cornell University Press: Ithaca, NY, 1985.
(34) Alexander, S. *J. Phys. (Paris)* **1977**, *38*, 983.
(35) Chen, X.; Inganäs, O. *Synth. Met.* **1995**, *74*, 159.
(36) Ruokolainen, J.; Torkkeli, M.; Levon, K.; Serimaa, R.; ten Brinke, G.; Ikkala, O., unpublished manuscript.

MA0259665